This is a repository copy of *An application of multi-level DC-link converter for optimised permutation control of PV sources under partial shading*.

White Rose Research Online URL for this paper:
http://eprints.whiterose.ac.uk/83895/

Version: Accepted Version

An application of multi-level DC-link converter for optimised permutation control of PV sources under partial shading

I Abdalla, J Corda, L Zhang

School of Electronic and Electrical Engineering, University of Leeds
Leeds LS2 9JT, United Kingdom
E-mail: l.zhang@leeds.ac.uk

Keywords: photovoltaic partial shading; maximum power point; multi-level converter;.

Abstract

The paper describes application of a multi-level DC-link converter in overcoming the problem of partially shaded series-connected PV sources. The converter control engages a permutation algorithm which enables each PV source of the string to produce the maximum power. The main features of the system are: (i) a continual operation of all PV sources, shaded and non-shaded, at their maximum power points, (ii) delivery of all extracted power from PV sources to the load and (ii) generation of multi-level output voltage waveform with a low total harmonic distortion.

1   Introduction

Partial shading of an array of photo-voltaic (PV) sources is a well-known problem which is manifested as a disproportionate reduction of electrical power generated from the array. This is caused by reduction of the current generated by the shaded source/s, which in turn becomes a limiting value of the current for the whole series string including the non-shaded sources.

The most common and rudimentary remedy for this problem is inclusion of bypassing diodes which temporarily eliminate shaded sources in the array, but this causes a significant reduction of power generated from the PV array. More sophisticated methods for solving the problem of partial shading, such as for example methods discussed in [1, 2], are based on avoiding direct connections of individual PV sources by using power electronic converters, which results in better utilisation of PV sources within the array.

The emerging method in dealing with the partial shading problem is based on connecting PV sources into the topology of a multi-level converter, which enables control of each PV source individually. In [3], for example, this concept has been described using five-level H-bridge converter with two PV sources. Since each PV source was emulated by a voltage source connected in series with a resistor, the experiment has not reflected the correct PV response particularly under partial shading. In another example [4], a multi-level diode-clamped converter is used to extract the power from each PV

source separately. The experimental results showed that the total achieved power was delivered completely to the load, but it has not been shown if all PV sources operated at individual maximum power point (MPP). In [5], the principles of controlling a multi-level DC-link converter through a novel algorithm based on the permutation of PV sources, is presented. The algorithm ensures that all PV sources of the string operate at their individual MPP under non-uniform irradiance. In the current paper, a modification is made in the PV permutation algorithm resulting in the quality improvement of the output.

2   Permutation Algorithm

In the topology shown in Fig.1 each PV unit consists of a single PV source, a capacitor, a switch and a diode. Units are connected in series and any of them can be switched in or out of the chain via its switch. These switches (SW1, SW2, SW3) operate at a high switching frequency and are controlled by the direct PWM method [6] to form the multi-level DC link waveform. (When a unit is switched off, it is being bypassed by a diode.) The H–bridge inverter at the output serves to produce alternative positive and negative output voltage half-cycles of the required output frequency. The generation of multiple voltage levels, combined with proper control, enables forming the approximate sinewave output. The control unit includes a perturbation and observation (P&O) MPPT block for each PV source. These provide a separate P&O tracking algorithm and the PI control for each PV source. The output signals of these blocks are multiplied by unity sinusoidal signal to form AC reference signals v_{ref1}, v_{ref2}, v_{ref3} for the control of the output H-bridge inverter.

All PV sources are sequentially permutated through consecutive PWM switching cycles according to the numerical count (C) as illustrated in Fig.2. The PV source which sequentially comes in turn at the highest voltage level is the only one which is controlled at a particular switching cycle (T_s), while other sources are used to build the appropriate voltage level. The benefits of such a process are: (i) all PV sources of the system are equally engaged and the switching losses of transistors associated with each PV source are balanced, (ii) the achievement of symmetrical positive and negative half-cycles of the output waveform under partial shading and (iii) the reduction of the voltage ripple on capacitors of PV units.
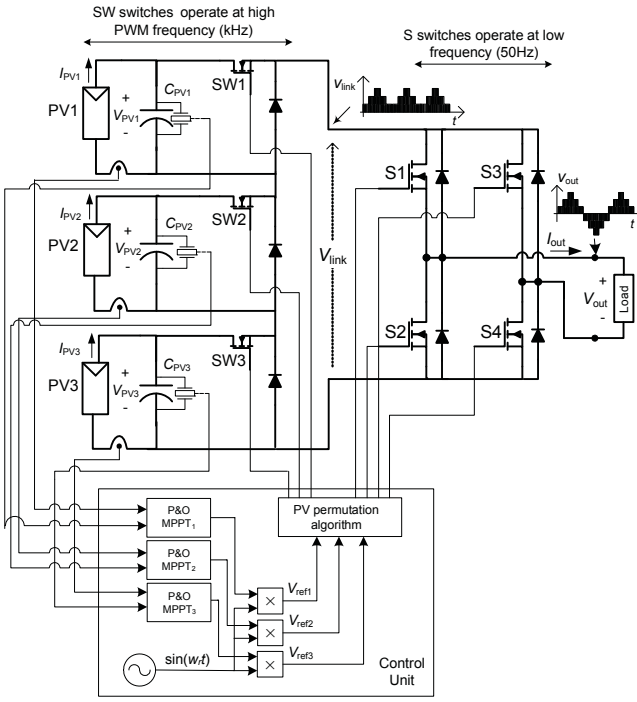
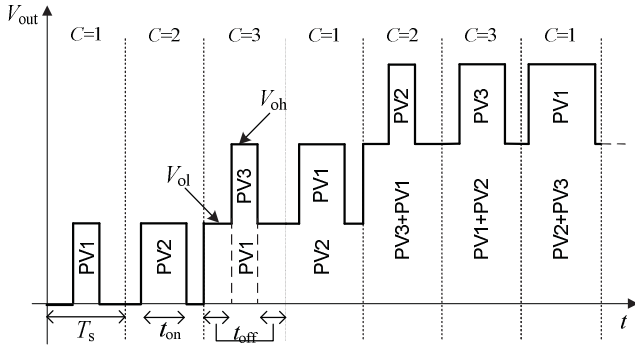Fig. 1: PV system controlled via multi-level converter

Fig. 2: Permutation of PV sources through consecutive PWM switching cycles

The direct PWM is used for determining the required lower and higher output voltage levels (V_{ol} and V_{oh}) and their time intervals (t_{off} and t_{on}) within each PWM switching interval of period T_s.

The direct PWM normalized reference voltage is given as:

$$\bar{v}_{\text{ref}(j)} = \frac{|v_{\text{ref}(j)}|}{V_L} \qquad (1)$$

where V_L denotes the MPP voltage at irradiance of 1000 W/m^2 and $j = 1, 2, \ldots n$ is the PV source index.

The integer part of the normalized reference voltage is defined as the normalized offset voltage, and it is given as

$$v_{\text{offset}(j)} = \text{int}\left[\bar{v}_{\text{ref}(j)}\right] \qquad (2)$$

The t_{on} interval of the PV source which is being controlled at a particular switching period, is given as

$$t_{\text{on}(j)} = T_s \cdot \left(\bar{v}_{\text{ref}(j)} - v_{\text{offset}(j)}\right) \qquad (3)$$

Table 1 illustrates the PV output generation stage of the algorithm in the basic system with two PV sources. If $C=1$, the PV1 source is controlled by applying the direct PWM to v_{ref1} to find the required t_{on} time. The role of v_{ref2} is to determine V_{ol} by checking v_{offset2}. When $C=2$, the PV2 is controlled through v_{ref2}, and v_{ref1} is used to determine V_{ol}.

Unlike the basic algorithm [5], the improved algorithm does not represent the PV source at the output if its offset voltage is zero, except in the case when all offset voltages are zero. The reason for introducing this exception is to initiate the control and it is also required in the case of low PWM reference signals. Referring to Table 1, if $C=1$, $V_{\text{offset1}}=0$ and $V_{\text{offset2}}=1$, then V_{PV1} will not be presented at the output and the output is only represented by V_{PV2} for the time period T_s. Even though there is no control for PV1 source for this time interval, the bypass capacitor C_{PV1} is charging for the entire period T_s, which enables V_{PV1} to recover so that a series connection is avoided for the time interval t_{on} when the source PV1 is shaded.

C	$v_{\text{offset 1}}$	$v_{\text{offset 2}}$	Output generation per switching period T_s
1	0	0	
	1	0	
	0	1	
	1	1	
2	0	0	
	0	1	
	1	0	
	1	1	

Table 1: The output generation from two PV sources

The process of generating the output waveform in the basic system with two PV sources (five-level DC-link converter) is graphically illustrated in the Appendix.

Table 2 shows the output generation stage of the algorithm for the case of three PV sources ($n = 3$) as a function of the offset voltages.

C	$v_{offset1}$	$v_{offset2}$	$v_{offset3}$	V_{ol}	V_{oh}	t_{on}
1	0	0	0	0	V_{PV1}	t_{on1}
	0	0	1	0	0	
	0	0	2	V_{PV3}	V_{PV3}	
	0	1	0	V_{PV2}	V_{PV2}	
	0	1	1	V_{PV2}	V_{PV2}	
	0	1	2	$V_{PV2}+V_{PV3}$	$V_{PV2}+V_{PV3}$	
	0	2	0	V_{PV2}	V_{PV2}	
	0	2	1	$V_{PV2}+V_{PV3}$	$V_{PV2}+V_{PV3}$	
	0	2	2	$V_{PV2}+V_{PV3}$	$V_{PV2}+V_{PV3}$	
	1	0	0	0	V_{PV1}	
	1	0	1	0	V_{PV1}	
	1	0	2	V_{PV3}	$V_{PV1}+V_{PV3}$	
	1	1	0	V_{PV2}	$V_{PV1}+V_{PV2}$	
	1	1	1	V_{PV2}	$V_{PV1}+V_{PV2}$	
	1	1	2	$V_{PV2}+V_{PV3}$	$V_{PV1}+V_{PV2}+V_{PV3}$	
	1	2	0	V_{PV2}	$V_{PV1}+V_{PV2}$	
	1	2	1	$V_{PV2}+V_{PV3}$	$V_{PV1}+V_{PV2}+V_{PV3}$	
	1	2	2	$V_{PV2}+V_{PV3}$	$V_{PV1}+V_{PV2}+V_{PV3}$	
	2	0	0	0	V_{PV1}	
	2	0	1	V_{PV3}	$V_{PV1}+V_{PV3}$	
	2	0	2	V_{PV3}	$V_{PV1}+V_{PV3}$	
	2	1	0	V_{PV2}	$V_{PV1}+V_{PV2}$	
	2	1	1	$V_{PV2}+V_{PV3}$	$V_{PV1}+V_{PV2}+V_{PV3}$	
	2	1	2	$V_{PV2}+V_{PV3}$	$V_{PV1}+V_{PV2}+V_{PV3}$	
	2	2	0	V_{PV2}	$V_{PV1}+V_{PV2}$	
	2	2	1	$V_{PV2}+V_{PV3}$	$V_{PV1}+V_{PV2}+V_{PV3}$	
	2	2	2	$V_{PV2}+V_{PV3}$	$V_{PV1}+V_{PV2}+V_{PV3}$	
2	0	0	0	0	V_{PV2}	t_{on2}
	0	0	1	V_{PV3}	V_{PV3}	
	0	0	2	V_{PV3}	V_{PV3}	
	0	1	0	0	V_{PV2}	
	0	1	1	V_{PV3}	$V_{PV2}+V_{PV3}$	
	0	1	2	V_{PV3}	$V_{PV2}+V_{PV3}$	
	0	2	0	0	V_{PV2}	
	0	2	1	V_{PV3}	$V_{PV2}+V_{PV3}$	
	0	2	2	V_{PV3}	$V_{PV2}+V_{PV3}$	
	1	0	0	0	0	
	1	0	1	V_{PV3}	V_{PV3}	
	1	0	2	$V_{PV1}+V_{PV3}$	$V_{PV1}+V_{PV3}$	
	1	1	0	0	V_{PV2}	
	1	1	1	V_{PV3}	$V_{PV2}+V_{PV3}$	
	1	1	2	$V_{PV1}+V_{PV3}$	$V_{PV1}+V_{PV2}+V_{PV3}$	
	1	2	0	V_{PV1}	$V_{PV1}+V_{PV2}$	
	1	2	1	$V_{PV1}+V_{PV3}$	$V_{PV1}+V_{PV2}+V_{PV3}$	
	1	2	2	$V_{PV1}+V_{PV3}$	$V_{PV1}+V_{PV2}+V_{PV3}$	
	2	0	0	V_{PV1}	V_{PV1}	
	2	0	1	$V_{PV1}+V_{PV3}$	$V_{PV1}+V_{PV3}$	
	2	0	2	$V_{PV1}+V_{PV3}$	$V_{PV1}+V_{PV3}$	
	2	1	0	V_{PV1}	$V_{PV1}+V_{PV2}$	
	2	1	1	$V_{PV1}+V_{PV3}$	$V_{PV1}+V_{PV2}+V_{PV3}$	
	2	1	2	$V_{PV1}+V_{PV3}$	$V_{PV1}+V_{PV2}+V_{PV3}$	
	2	2	0	V_{PV1}	$V_{PV1}+V_{PV2}$	
	2	2	1	$V_{PV1}+V_{PV3}$	$V_{PV1}+V_{PV2}+V_{PV3}$	
	2	2	2	$V_{PV1}+V_{PV3}$	$V_{PV1}+V_{PV2}+V_{PV3}$	

Continued ….

C	$v_{offset1}$	$v_{offset2}$	$v_{offset3}$	V_{ol}	V_{oh}	t_{on}
3	0	0	0	0	V_{PV3}	t_{on3}
	0	0	1	0	V_{PV3}	
	0	0	2	0	V_{PV3}	
	0	1	0	0	0	
	0	1	1	0	V_{PV3}	
	0	1	2	V_{PV2}	$V_{PV2}+V_{PV3}$	
	0	2	0	V_{PV2}	V_{PV2}	
	0	2	1	V_{PV2}	$V_{PV2}+V_{PV3}$	
	0	2	2	V_{PV2}	$V_{PV2}+V_{PV3}$	
	1	0	0	V_{PV1}	V_{PV1}	
	1	0	1	V_{PV1}	$V_{PV1}+V_{PV3}$	
	1	0	2	V_{PV1}	$V_{PV1}+V_{PV3}$	
	1	1	0	V_{PV1}	V_{PV1}	
	1	1	1	V_{PV1}	$V_{PV1}+V_{PV3}$	
	1	1	2	$V_{PV1}+V_{PV2}$	$V_{PV1}+V_{PV2}+V_{PV3}$	
	1	2	0	$V_{PV1}+V_{PV2}$	$V_{PV1}+V_{PV2}$	
	1	2	1	$V_{PV1}+V_{PV2}$	$V_{PV1}+V_{PV2}+V_{PV3}$	
	1	2	2	$V_{PV1}+V_{PV2}$	$V_{PV1}+V_{PV2}+V_{PV3}$	
	2	0	0	V_{PV1}	V_{PV1}	
	2	0	1	V_{PV1}	$V_{PV1}+V_{PV3}$	
	2	0	2	V_{PV1}	$V_{PV1}+V_{PV3}$	
	2	1	0	$V_{PV1}+V_{PV2}$	$V_{PV1}+V_{PV2}$	
	2	1	1	$V_{PV1}+V_{PV2}$	$V_{PV1}+V_{PV2}+V_{PV3}$	
	2	1	2	$V_{PV1}+V_{PV2}$	$V_{PV1}+V_{PV2}+V_{PV3}$	
	2	2	0	$V_{PV1}+V_{PV2}$	$V_{PV1}+V_{PV2}$	
	2	2	1	$V_{PV1}+V_{PV2}$	$V_{PV1}+V_{PV2}+V_{PV3}$	
	2	2	2	$V_{PV1}+V_{PV2}$	$V_{PV1}+V_{PV2}+V_{PV3}$	

Table 2: The output voltage generation from three PV sources

3 Simulation of the System Performance

To compare the improved algorithm with its precursor [5], the Fast Fourier Transformation (FFT) is applied to the output waveform to find the voltage spectrum and the total harmonics distortion (THD) which is calculated for the first thousand harmonics. The waveforms were simulated for the five and seven-level DC-link converters operating in the PV system with parameters given in Table 3. The I-V characteristics of the PV source at different irradiances were derived by Bishop's model and are shown in Fig.3.

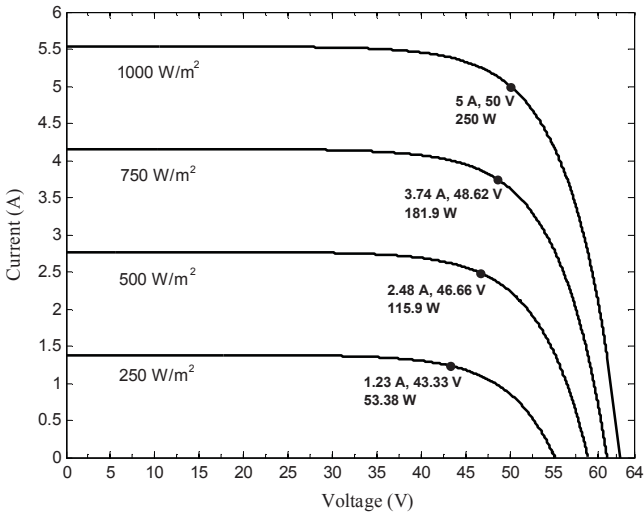| Parameter	Quantity	Value
P_{mpp}	PV source maximum power	250W
R_l	Load resistance	8.5Ω 7-level 18.5Ω 9-level 23Ω 11-level
e_v	P&O tracking step size	0.5V
M_f	Frequency modulation index	300
K_p	Proportional quiescent	0.1
K_i	Integration quiescent	100
f_r	AC output frequency	50Hz
C_{pv}	PV source bypass capacitor	5500µF

Table 3: PV system parameters

Fig. 3: I-V characteristics of the PV source for different irradiance levels. (MPP is indicated on each characteristic.)

Referring to Fig.4a, which relates to the five-level converter with sources PV1 and PV2 exposed to irradiances of 500 and 1000 W/m² respectively, the improved algorithm gave better voltage waveform (shown on the right) compared with the precursor algorithm. The THD of 43.52% and the 50-Hz fundamental peak voltage $V_{1(p)}$=76.81V was achieved with the improved algorithm, while THD=58.65% and $V_{1(p)}$=70.72V was achieved with the precursor. In Fig.4b the irradiances 750 and 500 W/m² were applied to PV1 and PV2 respectively. THD of 50.07% and $V_{1(p)}$=68.67V are achieved by the improved algorithm, compared with THD of 80.37% and $V_{1(p)}$=57.66V by the precursor.
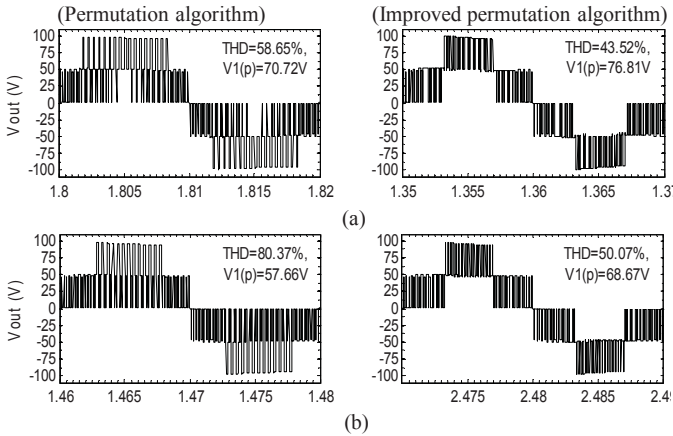

Fig. 4: Simulated five-level output waveforms produced by the precursor algorithm and the improved algorithm under irradiances applied to PV1 and PV2 respectively: (a) 500 and 1000 W/m²; (b) 750 and 500 W/m².

Similar comparison was made for the seven-level converter operating with three PV sources. At irradiances of 1000, 500 and 1000W/m² applied to PV1, PV2 and PV3 respectively (Fig.5a), the improved algorithm generates substantially better output waveform (THD=35.72%, $V_{1(p)}$=108.64V) compared to the waveform achieved with the precursor (THD=57.41%, $V_{1(p)}$=95.81V). When the irradiances of 250, 750 and 1000W/m² are applied to the PV1, PV2 and PV3 respectively (Fig.5b), the voltage waveform resulting from the improved algorithm has THD=42.52% and $V_{1(p)}$=94.04V, while with the precursor THD=58.02% and $V_{1(p)}$=89.62V.
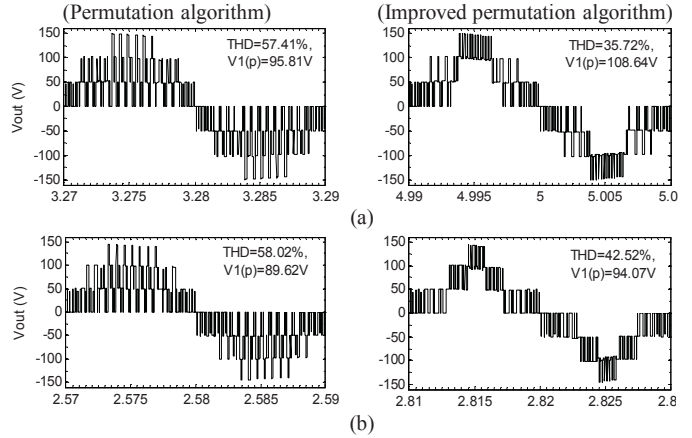

Fig. 5: Simulated seven-level output voltage waveforms produced by the precursor algorithm and the improved algorithm under irradiances applied to PV1, PV2 and PV3 respectively: (a) 100, 500 and 1000 W/m²; (b) 250, 750 and 1000 W/m².

The performance of the PV system using the improved algorithm was also simulated under dynamic irradiance. The system showed ability to track the MPP of each PV source without affecting other PV sources. Fig.6 illustrates the extracted power from each PV source and the total power delivered to the load from the seven-level converter for a sequence of events in terms of the irradiance variations. Initially the full irradiance (1000 W/m²) is applied to all three PV sources, so the extracted power from each source is 250W and a total power of 750 W is delivered to the load. In the time between 2 and 5 seconds, the irradiance to PV3 source is halved, while PV1 and PV2 are still at full irradiance. The extracted power from PV3 is now reduced to 116 W which matches the MPP on I-V characteristic of Fig.3 at 50% shading, i.e. at the irradiance of 500 W/m². The power of PV1 and PV2 are not affected by the shading of PV3, so the total delivered power is 616 W. During the time interval between 5 and 8 seconds, both PV2 and PV3 are shaded at the halved irradiance (500 W/m²) while PV1 is under the full irradiance, and the delivered power is 482 W. During the time interval between 8 and 11 seconds, all three PV sources are operated shaded to the halved irradiance (500 W/m²), and the power delivered to the load is reduced to 348 W. After 11 seconds all three PV sources are again exposed to the full irradiance and are recovered to their MPPs of 250 W delivering the total power of 750 W.
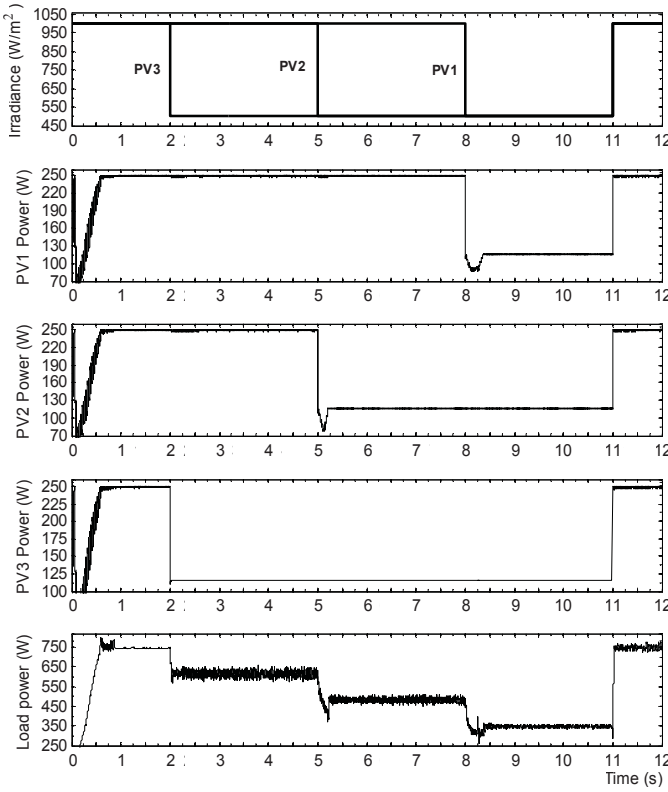
Fig. 6: Irradiance waveforms, the extracted power of PV1, PV2, PV3, and the load power of the seven-level DC-link converter

4 Conclusions

The main features of the developed PV system, which uses the improved permutation algorithm, are: (i) the upholding of operation of all PV sources (shaded and non shaded) at their MPPs, (ii) the delivery of all extracted power from PV sources to the load and (ii) the generation of improved multi-level voltage waveforms with low THD.

The proposed system was simulated using the Matlab–Simulink for five and seven-level DC-link converter. The comparison between the previous and the improved permutation algorithm have shown that the latter generates a lower distortion of the output waveform and a higher amplitude of the fundamental harmonic of the output voltage.

The time varying irradiance levels were applied to test dynamic behaviour of the system in terms of the MPP tracking. The algorithm enables each shaded PV source to be recovered to its MPP without affecting other PV sources in the circuit.

Appendix

When $C = 1$:

If $v_{offset1}$ is either 0 or 1 and $v_{offset2} = 0$, then:
    SW1 is 'on' during interval t_{on1} and 'off' otherwise;
    SW2 is 'off' during entire period T_s.

If $v_{offset1} = 0$ and $v_{offset2} = 1$, then:
    SW1 is 'off' and SW2 is 'on' during entire period T_s.

If $v_{offset1} = 1$ and $v_{offset2} = 1$, then:
    SW1 is 'on' during interval t_{on1} and 'off' otherwise;
    SW2 is 'on' during entire period T_s.

When $C = 2$:

If $v_{offset2}$ is either 0 or 1 and $v_{offset1} = 0$, then:
    SW1 is 'off' during entire period T_s;
    SW2 is 'on' during interval t_{on2} and 'off' otherwise.

If $v_{offset2}$ is 0 and $v_{offset1} = 1$, then:
    SW2 is 'off' and SW1 is 'on' during entire period T_s.

If $v_{offset1} = 1$ and $v_{offset2} = 1$, then:
    SW1 is 'on' during entire period T_s;
    SW2 is 'on' during interval t_{on2} and 'off' otherwise.

In Fig.1A, v_{ref1} and v_{ref2} are two reference voltages of the five-level inverter. These signals are sampled at intervals T_s yielding M_f samples for each reference signal over the time period $T_r (= 1/f_r)$. At each interval T_s, the sampled values are applied to the Eqs.(1) - (3) for generating the required control signals.
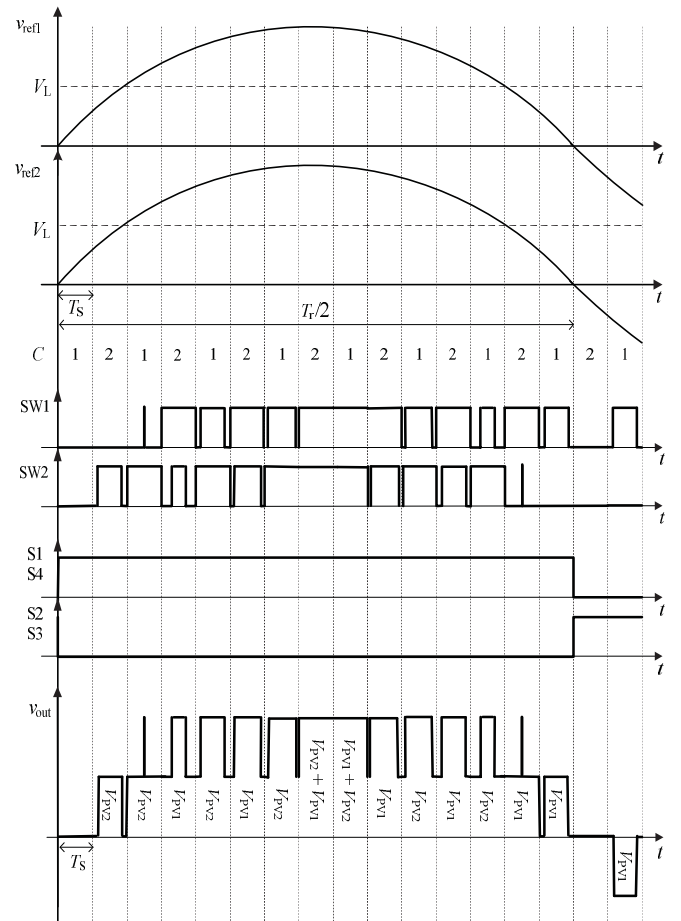

Fig. 1A: The waveform generating process by the improved PV permutation algorithm for five-level converter

5

References

[1] T. Shimizu, M. Hirakata, T. Kamezawa, H. Watanabe, "Generation control circuit for photovoltaic modules", *IEEE Trans. Power Electronics*, Vol.16, No.3, pp.293-300, May 2001.

[2] G. R. Walker, P. C. Sernia, "Cascaded DC-DC converter connection of photovoltaic modules", *IEEE Trans. Power Electronics*, Vol.19, No.4, pp.1130-1139, July 2004.

[3] S. J. Lee, H. S. Bae, B. H. Cho, "Modeling and control ofthe single-phase photovoltaic grid-connected cascaded H-bridge multilevel inverter", *IEEE Energy Conversion Congress (ECCE'09)*, pp.43-47, (2009).

[4] S. Busquets-Monge, J. Rocabert, P. Rodriguez, S. Alepuz, J. Bordonau, "Multilevel diode-clamped converter for photovoltaic generators with independent voltage control of each solar array", *IEEE Trans. Industrial Electronics*, Vol.55, No.7, pp.2713-2723, July 2008.

[5] I. Abdalla, J. Corda, L. Zhang, "Multilevel DC-Link Inverter and Control Algorithm to Overcome the PV Partial Shading", *IEEE Trans. Power Electronics*, Vol.28, No.1, pp.14-18, Jan.2013.

[6] D. Ning-Yi, W. Man-Chung, C.Yuan-Hua, H.Ying-Duo, "A 3-D generalized direct PWM algorithm for multilevel converters", *IEEE Letters. Power Electronics*, Vol.3, No.3, pp.85-88, 2005.